

## A quantum mechanical study using the density functional theory DFT/B3LYP and PCM model on the effects of polar solvent on the structure, stability and infrared vibration modes and spectrum of three hydroxyl benzene

Essam Nasser<sup>1</sup>, Dr.Nabil Joudieh<sup>2</sup>

Dr. Khansaa Hussein<sup>3</sup>

1. Faculty of Pharmacy – International University for Science and Technology, Ghabgeb – Daraa

2. Assistant Professor, Department of Physics - Faculty of Science - University of Damascus

3. Professor of Chemistry Department - Faculty of Science - University of Damascus

### Abstract

A theoretical investigation concerning the three hydroxyl benzene isomers in both gas and liquid phases have been carried out. Optimization geometry, relative stability energy, Infrared spectra for all possible isomers have been made using Density Functional Theory DFT/B3LYP basis set. The effect of solvent on the energy thermodynamic factors out infrared spectra have been determined using polarized continuum model PCM. Total free energy in the solution, cavitation energy, dispersion energy including repulsion energy and total non-electrostatic energy have been calculated using self-consistent field theory. The obtained results show a consistent between calculated and theoretical infrared spectra using both DFT/B3LYP and PCM level of calculation in both gas and liquid phases. The results confirm also the role of solvation on the stability of molecules.

Received :2022/04/13

Accepted:2022/07/04



**Copyright:** Damascus University- Syria, The authors retain the copyright under a CC BY- NC-SA

**Keywords:** Density Functional Theory, PCM Theory, Molecular Modeling, Relative Stability, Transition State, Theoretical IR Spectrum, Vibration Modes, solvent effects, Cavitation Energy, Dispersion Energy, Repulsion Energy, SCF PCM corrected Energy, Benzenetriols conformers.

## دراسة كمومية باستعمال نظرية تابع الكثافة DFT/B3LYP ونموذج الانحلال PCM لتأثير بعض المحلات القطبية على بنية واستقرار وأنماط اهتزاز طيف تحت الأحمر لمتماكات ثلاثي هيدروكسيل البنزن

عصام الناصر<sup>1</sup>، د. نبيل جودية<sup>2</sup>، د. خنساء حسين<sup>3</sup>

1. كلية الصيدلة - الجامعة الدولية الخاصة للعلوم والتكنولوجيا- غياغب- درعا

2. أستاذ مساعد في قسم الفيزياء - كلية العلوم - جامعة دمشق

3. أستاذ قسم الكيمياء - كلية العلوم - جامعة دمشق

### الملخص:

حددت الهندسة الفضلى، وطاقة الاستقرار النسبي، وأطياف تحت الأحمر لجميع متماكات ثلاثي هيدروكسيل البنزن بطريقة كمومية بالاستناد إلى نظرية تابع الكثافة DFT/B3LYP. تُرس كذلك تأثير المذيب على كلٍ من الهندسة الفضلى، والطاقة، والتوابع الترموديناميكية وأطياف تحت الأحمر باستخدام نظرية النموذج المستقطب المستمر (Polarized Continuum Model) المعروفة باسم PCM وحُددت أيضاً جميع الكميات الترموديناميكية النظرية المعرفة لظاهرة التذوب (Solvation) مثل الطاقة الحرة الكلية في المحلول، وطاقة الوضع في الحجرة (Cavitation Energy)، وطاقة التبعثر (Dispersion Energy)، وطاقة التدافع، والطاقة الكلية اللا كهروساكنة والتصحيح على طاقة الحقل التوافق الذاتي SCF (Self-Consistent Field) الناتج عن عملية التذوب. لوحظ توافق جيد جداً بين أطياف تحت الأحمر النظرية والتجريبية مما يشير إلى صلاحية طريقتي DFT/B3LYP و PCM لوصف وتمييز وتفسير هذه المتماكات في الطورين الغازي والسائل، إضافة إلى التأكيد على الدور المهم لعملية التذوب فيما يتعلق باستقرار الجزيئات وخصائصها البنوية والطيفية.

الكلمات المفتاحية: نظرية تابع الكثافة، نظرية النموذج المستقطب المستمر، النمذجة الجزيئية، الاستقرار الطاقى النسبي، الحالة الإنتقالية، أطياف تحت الأحمر النظرية، أنماط الاهتزاز، أفعال المذيب، طاقات الوضع في حُجيرة والتبعثر والتدافع وذاتية الترابط بوجود المذيب، متماكات ثلاثي هيدروكسيل البنزن.

تاريخ الإيداع: 2022/4/13

تاريخ الموافقة: 2022/07/04



حقوق النشر: جامعة دمشق -

سورية، يحتفظ المؤلفون بحقوق

النشر بموجب الترخيص

CC BY-NC-SA 04

## 1- Introduction

Trihydroxybenzenes contain pyrogallol (1,2,3-trihydroxybenzene), hydroxyquinol (1,2,4-trihydroxybenzene), and phloroglucinol (1,3,5-trihydroxybenzene). It's a part from the wide family of compounds named Phenolic compounds [1-2]. These compounds are known to exhibit various biological activities such as antimicrobial, antioxidant and anti-inflammatory properties. It is useful for the industrial synthesis of pharmaceuticals (Flopropione), Phloretin, and explosives (TATB (2,4,6-triamino- 1,3,5 trinitrobenzene), trinitrophenol, 1,3,5-trinitrobenzene). The theoretical study on the Trihydroxybenzenes is still limited. In 2021, Mayhan and all [3] report a study on the proton affinities and gas-phase basicities of pyrogallol (1,2,3-trihydroxybenzene) and phloroglucinol (1,3,5-trihydroxybenzene), as determined by a high level quantum calculations and a series of isodesmic proton transfer reactions. The authors discuss also the preferred protonation sites and relative thermochemical values are analyzed in terms of electron delocalization effects and the consequent disruption of intramolecular hydrogen bonding. In 2019 Otukile and all [4] perform a theoretical investigation, at the DFT/M06-2X, DFT/MPW1K and DFT/BHLYP level, on the reactions of 1, 3, 5-trihydroxybenzene (PG) and 2, 4,6-trihydroxyacetophenone (ACPG) with  $\bullet\text{OOH}$  with the aim of elucidating the peroxy radical scavenging properties of PG and its acylated derivative. In 2002, Gier and all [5] report for the gas phase and at the CASSCF/CASMP2 level the results of calculations on the structure and vibrations of gaseous (1,2,3-trihydroxybenzene) in the ground and excited state. The authors report also the experimental R2PI spectra of this compound. While the Schiff bases are a modified structure of Trihydroxybenzenes, we report the study realized in 2015 by Rashee and all [6] who synthesized, identified by FTIR and ultraviolet-visible (UV-Visible) spectroscopy and performed an optimized structures at the B3LYP/6-31G level on the Schiff base ligand.

Based on the tools of molecular modeling, we study in both gas and liquid phases the stability, geometry and spectral properties of Trihydroxybenzenes and show the importance of solvent and intra and inter molecular interactions. Based on the very extensive study of Tirado-Rives [7] published in 2008 we will use in this work the most popular and reasonably accurate DFT/B3LYP Hybrid Density Function Theory. Except that the DFT method takes into account the electronic correlation and is less time-expensive method compared to more sophisticated methods such as Configuration Interaction (CI) or Many Body Perturbation Theory (MBPT or MPn), the paper by Tirado-Rives reinforce our choice. In fact, Tirado-Rives have been testing the commonly used hybrid density functional B3LYP with the 6-31G(d), 6-31G(d,p), and 6-31+G(d,p) basis sets and has been carried out the calculations for 622 neutral, closed-shell organic compounds containing the elements C, H, N, and O. The focus is comparison of computed and experimental heats of formation and isomerization energies of these compounds. We conclude that DFT/B3LYP give very accurate results for almost all fundamental structure of organic compounds. Motivated by testing a new base than the one used by Tirado-Rives and all, we use the atomic pseudo-potential determined in Toulouse [8] for the C and O atoms, because it is less time-expensive while being accurate for organic molecules. We think that this basis set is well adapted to our study because the structures studied contain a limited number of non-heavy atoms, and the compounds have a quasi-plan structure, so that the potential energy surface is without special complications and the optimization will go without problems. Concerning the liquid state effects, we take into account the solvent effects via the PCM model of solvation which is considered among the best of solvation models. Although the PCM model is computationally expensive, arising from complicated realistic cavity made of multiple of interlocking spheres, it has considerable advantages over the other solvation models, because it providing a more realistic shape of a cavity, taking into account the mutual polarization between the solute and the polarizable medium and considering dispersion energy in solute molecules having zero dipole moment.

## 2- Method of calculation

### 2-1 Basics of DFT theory

Molecular modeling [9,10] and his programs actually disponible forms a <quantometer> in that it permits to obtain and interprets the relative stability of species, energetic, thermodynamic and electromagnetic properties and diver's spectra such as NMR and IR spectra. The literature of the DFT theory is very extensive, but we found the fundamental in reference [11-21]. In 1964, Hohenberg and Kohn, based on the Thomas-Fermi model, proved the existence of the energy function  $E[\rho(\vec{r})]$ , which leads using the variation theory to the basic equations of the DFT theory [22]. The practical application of the DFT theory became possible through the of Kohn and Sham, who proposed in 1965 a set of single-electron equations similar to the Hartree-Fock equations that allow to obtain the electron density and energy of the molecule [23]. The

DFT theory is mainly based on the Hohenberg-Kohn theorems. The first theorem states that it is possible to determine the molecular energy, wave function, and all electronic properties from the electron density  $\rho_0(\vec{r})$  of the fundamental energy level [22]. The electronic density  $\rho(\vec{r})$  lead the knowledge of the determine the number of electrons, the external potential, and the total energy of the system, which is written as the product of the sum of three functions as follows:

$$E[\rho(\vec{r})] = V_{ne}[\rho(\vec{r})] + T[\rho(\vec{r})] + V_{ee}[\rho(\vec{r})] \quad (1)$$

$$V_{ne}[\rho(\vec{r})] = \int \rho(\vec{r}) \cdot V(\vec{r}) \cdot d^3\vec{r} \quad (2)$$

$$T[\rho(\vec{r})] = \int \left[ -\frac{1}{2} \cdot \nabla^2 \rho(\vec{r}) \right] \cdot d^3\vec{r} \quad (3)$$

$$J[\rho(\vec{r})] = \frac{1}{2} \iint \frac{1}{r_{12}} \cdot \rho(\vec{r}_1) \cdot \rho(\vec{r}_2) \cdot d^3\vec{r}_1 \cdot d^3\vec{r}_2 \quad (4)$$

$$K[\rho(\vec{r})] = \frac{1}{4} \iint \frac{1}{r_{12}} \cdot \rho(\vec{r}_1, \vec{r}_2) \cdot \rho(\vec{r}_1, \vec{r}_2) \cdot d^3\vec{r}_1 \cdot d^3\vec{r}_2 \quad (5)$$

$$V_{ee}[\rho(\vec{r})] = J[\rho(\vec{r})] + K[\rho(\vec{r})] \quad (6)$$

So, the energy functions can be written as:

$$E_0[\rho(\vec{r})] = \int \rho_0(\vec{r}) \cdot V(\vec{r}) \cdot d^3\vec{r} + F_{HK}[\rho_0(\vec{r})] \quad (7)$$

$$F_{HK}[\rho_0(\vec{r})] = T[\rho_0(\vec{r})] + V_{ee}[\rho_0(\vec{r})] \quad (8)$$

The functional  $F_{HK}[\rho_0]$  takes into account all inter-electronic interaction, and is independent of the external potential. Therefore,  $F_{HK}[\rho_0]$  is a functional suitable for studying any systems. Unfortunately, we do not yet know the exact mathematical form of this function and it is necessary to search for it an approximate form, and for this the second HK theorem was developed. It states that for variational density  $\tilde{\rho}(\vec{r})$  such that:

$$\tilde{\rho}(\vec{r}) > 0 \quad , \quad \int \tilde{\rho}(\vec{r}) \cdot d^3\vec{r} = n \quad (9)$$

the following inequalities come true

$$E_0 \leq \tilde{E}[\tilde{\rho}(\vec{r})] \quad (10)$$

Using the extremum condition applicable to the functional  $\tilde{E}[\tilde{\rho}(\vec{r})]$  and appropriate mathematical developments to the basic equation of the DFT theory:

$$\mu = \frac{\delta E[\rho(\vec{r})]}{\delta \rho(\vec{r})} = V(\vec{r}) + \frac{\delta F_{HK}[\rho(\vec{r})]}{\delta \rho(\vec{r})} \quad (11)$$

where  $\mu$  is the electronic chemical potential of the system.

## 2-2 Kohn-Sham Method

The Hohenberg-Kohn theorems do not allow us to obtain a procedure for calculating energy  $E_0$  from  $\rho(\vec{r})$  or calculating  $\rho(\vec{r})$  without prior knowledge of the wave function. To solve this problem, Kohn and Sham proposed in 1965 a method that enable the energy  $E_0$  to be obtained from  $\rho_0(\vec{r})$  [11-21]. Kohn and Sham assumed the existence of a virtual reference system S consisting of n free electrons, and then they reformulated the problem so that the reference system has the same electronic density of the fundamental state of real system. After performing the appropriate mathematics, we can write the fundamental equations of the Kohn-Sham theory as follows:

$$H_s = \sum_{i=1}^n \left[ -\frac{1}{2} \nabla_i^2 + V_s(\vec{r}_i) \right] = \sum_{i=1}^n h_i^{KS}(\vec{r}_i) \quad (12)$$

$$h_i^{KS}(\vec{r}_i) \cdot \Psi_i^{KS}(\vec{r}_i) = \varepsilon_i^{KS} \cdot \Psi_i^{KS}(\vec{r}_i) \quad (13)$$

where  $\Psi_i^{KS}(\vec{r}_i)$  is the Kohn-Sham orbital for electron  $i$ .

We consider  $\Delta T$  the kinetic energy difference between the real system and the reference system, while  $\Delta V$  expresses the difference between the real electron-electron repulsion and the coulombic repulsion between the two-point charge distributions, expressed as:

$$\Delta T = T[\rho(\vec{r})] - T_s[\rho(\vec{r})] \quad (14)$$

$$\Delta V_{ee} = V_{ee}[\rho] - \frac{1}{2} \iint \frac{\rho(\vec{r}_1) \cdot \rho(\vec{r}_2)}{r_{12}} \cdot d^3\vec{r}_1 \cdot d^3\vec{r}_2 \quad (15)$$

We write the energy of system as:

$$E[\rho] = \int \rho(\vec{r}) \cdot V(\vec{r}) \cdot d^3\vec{r} + T_s[\rho] + \frac{1}{2} \iint \frac{\rho(\vec{r}_1) \cdot \rho(\vec{r}_2)}{r_{12}} \cdot d^3\vec{r}_1 \cdot d^3\vec{r}_2 + \Delta T[\rho] + \Delta V_{ee}[\rho] \quad (16)$$

And we define the exchange correlation energy functional as follows:

$$E_{xc}[\rho] = \Delta T[\rho] + \Delta V_{ee}[\rho] \quad (17)$$

therefore

$$E[\rho] = \int \rho(\vec{r}) \cdot V(\vec{r}) \cdot d^3\vec{r} + T_s[\rho] + \frac{1}{2} \iint \frac{\rho(\vec{r}_1) \cdot \rho(\vec{r}_2)}{r_{12}} \cdot d^3\vec{r}_1 \cdot d^3\vec{r}_2 + E_{xc}[\rho] \quad (18)$$

In the DFT theory, the main problem remains the finding of a suitable approximation to the functional  $E_{xc}[\rho]$ . To find the Kohn-Sham orbitals we solve the eigenfunctions and values equation for one Kohn-Sham electron:

$$\left[ -\frac{1}{2} \nabla_i^2 - \sum_{\alpha} \frac{Z_{\alpha}}{r_{i\alpha}} + \int \frac{\rho(\vec{r}_2)}{r_{12}} d^3\vec{r}_2 + V_{xc}(\vec{r}_1) \right] \cdot \Psi_i^{KS}(\vec{r}_1) = \varepsilon_i^{KS} \cdot \Psi_i^{KS}(\vec{r}_1) \quad (19)$$

The exchange-correlation potential is defined by functional derivative:

$$V_{xc}(\vec{r}) = \frac{\partial E_{xc}[\rho(\vec{r})]}{\partial \rho(\vec{r})} \quad (20)$$

There are several approximations to determine the exchange-correlation potential. The Kohn-Sham orbitals, solutions of the Kohn-Sham eigenfunctions and values equations, determine the electronic density:

$$\rho_0(\vec{r}) = \rho_s(\vec{r}) = \sum_{i=1}^n |\Psi_i^{KS}|^2 \quad (21)$$

Then, we start the computation using a primitive density which permits to calculate the effective potential

$$V_{eff}(\vec{r}) = - \sum_{\alpha} \frac{Z_{\alpha}}{r_{1\alpha}} + \int \frac{\rho(\vec{r}_2)}{r_{12}} d^3\vec{r}_2 + V_{xc}(\vec{r}_1) \quad (22)$$

This effective potential in turn allows solving the eigenfunctions and values equations of Kohn-Sham:

$$\left[ -\frac{1}{2} \nabla_1^2 + V_{eff} \right] \cdot \Psi_i^{KS}(\vec{r}_1) = E_i^{KS} \cdot \Psi_i^{KS}(\vec{r}_1) \quad (23)$$

The procedure is repeated until convergence that is until the difference entre two consecutive electronic density be sufficiently small.

### 2-3 Method of hybrid functional B3LYP

After passing by several developments and approximations [24-31], among which are the LDA and Generalized gradient approximations, Beche, Lee, Yang and Parr formulate the efficient B3LYP (Beche 3 Parameters Lee-Yang-Parr) hybrid functional which is a three-parameter functional resulting from the combining of Local Beche and Hartree-Fock exchanges with gradient-corrected due to Lee, Yang and Parr:

$$E_{xc}^{B3LYP} = (1 - a_0 - a_x).E_x^{LDA} + a_0.E_x^{HF} + a_x.E_x^{B88} + a_c.E_c^{LYP} + (1 - a_c).E_c^{VWN} \quad (24)$$

The following values [32] were chosen for the parameters:

$$a_0 = 0.20 \quad , \quad a_x = 0.72 \quad , \quad a_c = 0.81$$

### 3- Models of solvation

Actually, Modern quantum chemical methods are very accurate and useful tools for understanding and prediction the nature of the interaction solvent-solute and decompose this interaction to his principal's components and predicting his importance on the stability, structure and spectra of molecular systems and reactional mechanisms. of decomposer interactions and for predicting chemical structures and molecular spectra. The accurate characterization of chemical activity and reactivity in the dense phase is also of great importance. Practically, there are two ways to describe the effect of the surrounding environment on a molecule, the implicit and the explicit methods.

In the implicit model of solvation, the solute is characterized by its wave function, which is affected by the dielectric constant of solvent, and treated quantum mechanically in the framework of Born-Oppenheimer approximation. However, the solution is treated as a continuous and homogeneous medium called the continuum dielectric. Among the several interactions occurring in the solute-surrounding medium system, only interactions of electrostatic origin are considered. Also, the model supposes that at equilibrium the solvent form un isotropic medium and treat uniquely the static case and no water molecules per se. there are several implicit models likes the Polarizable Continuum Model (PCM), Solvation Model "Density" (SMD), and the Conductor-like Screening Model (COSMO). By contrast, the explicit model describes the solvent molecules at the atomic level that is electronic and nuclear structure including. Furthermore, this model uses the concept of micro solvation in that only few solvent molecules placed around solute and charge transfer with solvent can occur. Taking into account the long time required for calculations, the explicit model is used mainly in molecular mechanics approaches. There are Two models. The first is the Micro-solvation model which use a few solvent molecules (1 to 3) put at chemically reasonable place. In this model, water molecule is put close to exchangeable protons (OH, NH2...). The second model is the Macro-solvation in which first (sometimes second) solvent layer put around the whole molecule. This model habitually coupled to a Molecular Dynamics simulation. The original idea of modeling the electrical interactions solute-solvent consist on placing the solute into a finite cavity date back to Kirhwood's [33] and Onsager's research regarding the study of the effect of the dissolution action on polar molecules [34-36]. The view point of Onsager, consist on treating the solute surrounding by the solvent molecules using quantum mechanical model as a molecule confined in a cavity plunged in a continuous medium. The Born model formulated in 1912 is one of the simplest implicit models, which is based on considering a point charge, a molecule with point-dipole polarizabilities inside a sphere, that model a charged solute placed in a spherical cavity of the solution [35], as shown in Figure (1).

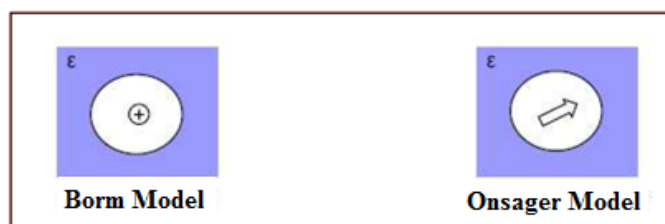
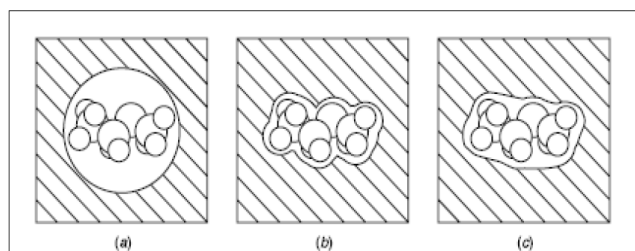


Figure (1): The implicit model of solvation

In 1936 Onsager generalized the Born model to a dipole moment placed in a spherical cavity of a solvent whose dielectric constant is  $\epsilon$ . The Onsager model of solvation is more general than Born one, because it is applicable to a wide range of molecules, including the charged species, while the Born model is limited only to charged systems. In this work, we use a variant of the implicit model, the Self-Consistent Reaction Field (SCRF) method. The SCRF is a method that calculate the effect of a polarizable solvent on the quantum system that is the solute. We suppose that the solvent is polarizable system and modeled as a dielectric continuum characterized by a dielectric constant. This dielectric continuum fills the space outside the quantum system (solute). The molecular surface is the boundary between the interior where the dielectric constant is unity, and the exterior. The charges of the solute cause polarization in the continuum giving rise to a reaction field which in turns affect the quantum system and modifies its electronic distribution. The reaction field is calculated through the resolution of Poisson equation combining to iterative self-consistency procedure between the reaction field and the charge distribution of quantum system. The profound root of the principals' ideas go back to Onsager model as mentioned previously and developed in the so-called PCM model of Tomasi and co-workers.

### 3-1 The Self-Consistent Reaction Field model (SCRF):

We first begin by describing the energy terms and energy balance of the continuous model of solvation, taking into account the various mutual interactions. The first step consists of creating a cavity in the continuous medium of the solvent, as shown in Figure (2).



**Figure (2): (a) a solute in spherical cavity in a continuous medium that have a dielectric constant . (b) cavity resulting from the unity of several atoms, with radius equal to Van Der Waals radius, composing the molecule (c) Cavity with surface disponible to solvent.**

In practice, the cavity is constructed from a group of spheres, representing the atoms of molecule, whose center is the nuclei of the dissolved atoms composed the molecule and whose radius is the order of the Van Der Waals radius. The formation of this cavity requires a quantity of positive energy  $\Delta G_{cav}$ , called the free energy of dissolution. this energy depends on the nature of the solvent and the topology of the cavity. In the next step, the solute is placed in the cavity and it reacts electrically with the dielectric continuous medium  $\epsilon$ . We usually distinguish three types of mutual interactions between the solute and the continuous medium, the electrostatic interaction represented by  $\Delta G_{elec}$ , the repulsive interaction and the scattering effects. The last two types of effects are calculated using approximate equations. We resume the mechanism of Self-Consistent Reaction Field (SCRF) of a dissolved molecule in a self-bonding cavity by the fact that the charge distribution of the solute polarizes the surface of the solvent cavity. This polarization leads in his turns to the apparition of electric charges on the surface of cavity. These charges creating an electric reaction, a field, that in turns modified the electronic distribution of solute. After this, the continuous medium is equilibrated by rearrangement, and this leads to a new distribution of electrical charges on the boundary of a solute-solvent medium, and this continues until an electrostatic equilibrium is reached between the charge distribution of the dissolved molecule and the charge distribution of the surface of the cavity. The always negative term describing this electrostatic contribution is  $\Delta G_{elec}$ .

In most cases, the precedent electrostatic contribution, describing the interaction between the boundary surface and the solute, is associated with a positive repulsive  $\Delta G_{rep}$  contribution and a negative dispersed  $\Delta G_{dis}$  contribution. Finally, the total energy of the mutual effects is written as the sum of one electrostatic term and three non-electrostatic terms as:

$$\Delta G_{solv} = \Delta G_{cav} + \Delta G_{elec} + \Delta G_{dis} + \Delta G_{rep} \quad (25)$$

This continuous medium model uses the Poisson equation in classical electrostatics in order to solve the problem:

$$-\vec{\nabla}[\varepsilon_r(\vec{r}) \cdot \vec{\nabla}V(\vec{r})] = 4\pi \cdot \rho_m(\vec{r}) \quad (26)$$

where  $\varepsilon_r(\vec{r})$  is the Dielectric Function of the continuous medium and  $V(\vec{r})$  is the total electrostatic potential which is the sum of two contributions:

$$V(\vec{r}) = V_\rho(\vec{r}) + V_\sigma(\vec{r}) \quad (27)$$

Where  $V_\rho(\vec{r})$  is the electrostatic potential due to the charge distribution of the electron-density  $\rho(\vec{r})$ , of the solute, and  $V_\sigma(\vec{r})$  is the reaction potential due to the polarization of the dielectric continuous medium. The function  $\varepsilon_r(\vec{r})$  is defined by the following relationship and can take two values:

$$\varepsilon_r(\vec{r}) = \frac{\varepsilon_s}{\varepsilon_0} = \begin{cases} 1 & \text{if } \vec{r} \in V_{int} \\ \varepsilon & \text{if } \vec{r} \in V_{ext} \end{cases} \quad (28)$$

Where, respectively,  $(V_{int}) V_{ext}$  is the volume inside (outside) the cavity. For both cases, the Poisson equation is written as:

$$-\vec{\nabla}^2 V(\vec{r}) = 4\pi \cdot \rho_m(\vec{r}) \quad \text{if } \vec{r} \in V_{int} \quad (29)$$

$$-\varepsilon \cdot \vec{\nabla}^2 V(\vec{r}) = 0 \quad \text{if } \vec{r} \in V_{ext} \quad (30)$$

Of course, the last two equations must be accompanied with the boundary conditions and the equations that describes the behavior of the potential at infinity, and those describing the limit conditions especially at the surface of the cavity, where  $|V_{int} - V_{ext}| = 0$ , in order to maintain the potential continuity. So, the surface distribution of charges  $\sigma_s(\vec{r})$  can be formulated in terms of calculable quantities:

$$\sigma(\vec{r}_s) = \frac{(\varepsilon - 1)}{4\pi \cdot \varepsilon} \cdot E(\vec{r}_s) \quad (31)$$

$$E(\vec{r}) = \left[ \frac{\partial V(\vec{r})}{\partial n} \right]_k \quad (32)$$

where  $E(\vec{r})$  is the electric field perpendicular to the surface of the cavity.

## 2-2 Continuous Polarization Model (PCM)

The PCM is a model that study the effect of the solvent using a cavity of a geometric shape closer to the reality than the sphere shape. It consists on dividing the surface of the cavity into very small primary surfaces composed of spherical polygons called Tesserae [37-39]. The surface of the Tesserae is taken small enough to take  $\sigma(\vec{r}_s)$  as a constant for each of these Tesserae. In this model, the solute molecule is placed in a cavity made up of a group of spheres nested one inside the other and centered around the atoms, as shown in Figure (3).

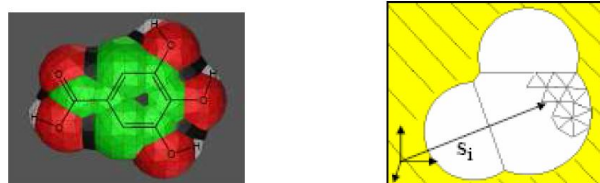


Figure (3): The cavity in the PCM

For each atom, each sphere is calculated in terms of the Van Der Waals radius for each atom, and the charge density is distributed over the surface of the cavity. In addition, the triangles at the intersection of two or more spheres are changed using a numerical algorithm that preserves the properties of the surface of the cavity and the charge distribution  $\sigma(\vec{r}_s)$  [40].

## 3-2-1 PCM algorithm

In the PCM model, the electronic wavefunction of the quantum system is determined from the zero-order electronic Hamiltonian to which an electrostatic term due to the presence of  $\sigma_s(\vec{r}_s)$  surface charges distribution on the interface between the solvent and the continuous medium are added. Then, the Hamiltonian in the presence of electric perturbations is written as:

$$\hat{H} = \hat{H}_0 + \hat{V}_\sigma \quad (33)$$

$$\hat{V}_\sigma(\vec{r}_s) = \int \frac{\sigma_s(\vec{r}_s)}{|\vec{r} - \vec{r}_s|} \cdot d\vec{r}_s \quad (34)$$

where  $\hat{H}_0$  is the electronic Hamiltonian in vacuum, and  $\hat{V}_\sigma$  is the electrostatic potential due to the solvent. In this case, the resolution of the eigenfunctions and eigenvalues problem of the perturbed Hamiltonian require an iterative self-consistent procedure. The calculation aims are to determine  $\sigma(\vec{r}_s)$  for each Tesserae using the surface  $\Delta S_k$  and the charge  $q_k$  at the point  $\vec{r}_k$  according to the relationship:

$$q_k = \sigma(\vec{r}_k) \cdot \Delta S_k \quad (35)$$

The iterative calculation is carried out according to the following step:

The first step:

We start from a primitive value of  $\sigma(\vec{r}_k)$  corresponding to a potential due to the charge distribution of the solute only, so  $V_\sigma(\vec{r}) = 0$  then:

$$V(\vec{r}) = V_\rho(\vec{r}) \quad (36)$$

We call  $\sigma_k^{00}$  the surface charges corresponding to this approximation. The first index 0 denotes the point charges of the solute only (without the solvent), while the second index 0 denotes the beginning, that is for that the state:

$$V_\sigma(\vec{r}) = 0 \quad (37)$$

We have then,

$$\sigma_k^{00} = - \left[ \frac{\varepsilon - 1}{4\pi} \right] \cdot \left[ \frac{\partial V(\vec{r})}{\partial n} \right]_k \quad (38)$$

Thus, we get the relationship:

$$q_k^{00} = \sigma_k^{00}(s) \cdot \Delta S_k \quad (39)$$

These charges in the center of the surface elements generate an additional contribution to the potential and electric field terms, and this allows the relationship to be written:

$$V^{00}(\vec{r}) = V_\rho^{00}(\vec{r}) + V_\sigma^{00}(\vec{r}) \quad (40)$$

The new distribution of surface charges  $\sigma_k^{01}$  and the associated charge can now be calculated using the equations:

$$\sigma_k^{01} = - \left[ \frac{\varepsilon - 1}{4\pi} \right] \cdot \left[ \frac{\partial V(\vec{r}_s)}{\partial n} \right]_k \quad (41)$$

$$q_k^{01} = \sigma_k^{01}(s) \cdot \Delta S_k \quad (42)$$

We continue the iterative calculation until we reach the convergence for which  $V_\sigma^{0f}(\vec{r})$  is obtained from the charges  $\sigma_k^{0f}$ . Then, the potential  $V_\sigma(\vec{r})$  can be added to the electronic Hamiltonian  $\hat{H}_0$  of the solute:

$$\hat{H} = \hat{H}_0 + \hat{V}_\sigma \quad (42)$$

It is then possible, depending on the quantum mechanical method to be used, to solve either the Hartree-Fock equations or the density functional theory equations using this Hamiltonian.

### Second step

So, the previous step leads to obtaining the new distribution of charges for the dissolved molecule, from which the new set of surface charges  $q_k^{10}$  can be obtained, and the process is repeated iteratively until obtaining  $q_k^{1f}$ , and then  $V_\sigma^{1f}(\vec{r})$ .

The same procedure is repeated until the global convergence is reached, and then obtaining the wave function  $\Psi^f$ . It is known that charges placed in vacuum (dielectric constant  $\epsilon_0$ ) create an electric field  $\vec{E}_0$  at point  $\vec{r}$  in space. In the solvent, characterized by the dielectric constant  $\epsilon_s$ , these charges in space create an additional electric field  $\vec{E}_s$ . We can calculate the change in the free energy of the system when passing from vide to solution using the equation:

$$\Delta G_{elec} = -\frac{1}{2} \left[ \iiint_{space} \epsilon_s(\vec{r}) \cdot \vec{E}^2 \cdot d\tau - \iiint_{space} \epsilon_s(\vec{r}) \cdot \vec{E}_0^2 \cdot d\tau \right] \quad (43)$$

From the expressions  $V^{00}(\vec{r})$  and  $\sigma^{01}$  and assuming zero charge density outside the cavity, the integration can uniquely be performed only on the charge density inside the cavity. In this case, the expression  $\Delta G_{elec}$  is written as:

$$\Delta G_{elec} = -\frac{1}{2} \iiint_{cav} V_R(\vec{r}) \cdot \rho(\vec{r}) \cdot d^3\vec{r} \quad (44)$$

The last relation show that the free energy change is equal to the half of the energy of the interactions between charges with the reaction potential. So, it is sufficient to include the value of the reaction potential within the last relation.

### 3-2-2-Non electrostatic terms

We classified the non- electrostatic terms into three types: the cavity term, scattering term and the repulsion term.

**A-** Cavity term: It is possible to suppose that the process of passing the molecule from the gas phase to the liquid phase as taking place in two steps which leads to an increase in free energy. The cavity is formed in the first step which is represented by the cavity term that have an experimental equivalent, which makes it difficult to compare different values resulting from different models calculating  $\Delta G_{cav}$ . The second term, represent the introduction of the solute into the cavity.

Pierotti [41] summarizes the calculation of the free energy of the cavity formation process by the following equation:

$$G_{cav} = \sum_i \frac{a_i}{4\pi R_i^2} \cdot [K_0 + K_1 \cdot (R_i + R_s) + K_2 \cdot (R_i + R_s)^2] \quad (45)$$

Where, respectively,  $i$  is the number of Tesseræ,  $a_i$  expresses the surface of the Tesseræ,  $R_i$  the radius of the associated sphere of the Tesseræ,  $R_s$  is the radius of the dissolved molecule, while  $K_0$  represent the surface tension, and  $K_1$  and  $K_2$  expresses parameters known in the scientific literature [42].

**B-** The scattering and repulsion terms: For long distance, an attracted force, named Van der Waals, applies between the two atoms, whereas for small distance a repulsive force dominates between them.

Lennard-Jones [43] proposed a mathematical expression for the potential in terms of the distance between the two atoms, written as:

$$V(\vec{r}) = 4E_0 \left[ \left( \frac{r_0}{r} \right)^{12} - \left( \frac{r_0}{r} \right)^6 \right] \quad (46)$$

where  $r$  is the distance between the two atoms A and B,  $E_0$  is the bond energy in the molecule, and  $r_0$  is the minimal bond length. In  $V(\vec{r})$ , the first term represents the repulsion potential, while the second expresses the attractive term. In the PCM model, the free energy of scattering and repulsion is calculated using the two following relations suggested by Floris and colleagues [44]:

$$G_{dis} = \rho \cdot \sum_N \sum_M \sum_i \left[ -\frac{C_{MN}}{|\vec{r}_M - \vec{r}_i|^6} + \frac{R_i^2 + |\vec{r}_M - \vec{r}_i|^6 - |\vec{r}_N - \vec{r}_i|^6}{2R_i} \cdot a_i \right] \quad (47)$$

$$G_{dis} = \rho \cdot \sum_N \sum_M \sum_i \left\{ \left[ \frac{1}{\alpha_{MN} \cdot |\vec{r}_M - \vec{r}_i|} + \frac{2}{\alpha_{MN}^2 \cdot |\vec{r}_M - \vec{r}_i|^2} + \frac{3}{\alpha_{MN}^3 \cdot |\vec{r}_M - \vec{r}_i|^3} \right] \cdot \beta_{MN} \cdot \exp(-\alpha_{MN} \cdot |\vec{r}_M - \vec{r}_i|) + \frac{R_i^2 + |\vec{r}_M - \vec{r}_i|^6 - |\vec{r}_N - \vec{r}_i|^6}{2R_i} \cdot a_i \right\} \quad (48)$$

where M is the number of atoms of the solution, N, the number of atoms of the solvent,  $i$  the number of Tesseractes,  $\rho$  is the density of the solution,  $C_{MN}$  is the scattering constant for the atoms of the solute M and the solvent N, and  $\alpha_{MN}, \beta_{MN}$  expressing the two parameters of the repulsive exponential potential between the M atom of the dissolved molecule and the N atom of the solvent. The vectors  $\vec{r}_M, \vec{r}_i$  represent the position vectors of the atom M and Tesseractes number  $i$ ,  $R_i$  expresses the radius of the accompanying sphere of Tesseractes. The  $a_i$  expresses the surface of the Tesseractes number. So, we can solve the eigenfunctions and values equation:

$$\hat{H}\Psi = (\hat{H}^0 + \hat{V}^R)\Psi = E\Psi \quad (49)$$

To find the free electrostatic energy  $G_{elec}$ :

$$G_{elec} = E - \frac{1}{2} \cdot \langle \Psi^f | \hat{V}^R | \Psi^f \rangle \quad (50)$$

$$G_{elec} = \langle \Psi^f | \hat{H}^0 | \Psi^f \rangle + \langle \Psi^f | \hat{V}^R | \Psi^f \rangle - \frac{1}{2} \cdot \langle \Psi^f | \hat{V}^R | \Psi^f \rangle \quad (51)$$

$$G_{elec} = \langle \Psi^f | \hat{H}^0 | \Psi^f \rangle + \frac{1}{2} \cdot \langle \Psi^f | \hat{V}^R | \Psi^f \rangle \quad (52)$$

So, the free energy of solvation is written as:

$$\Delta G_{elec} = G_{elec} - \langle \Psi^0 | \hat{H}^0 | \Psi^0 \rangle \quad (53)$$

$$\Delta G_{elec} = \langle \Psi^f | \hat{H}^0 | \Psi^f \rangle + \langle \Psi^0 | \hat{H}^0 | \Psi^0 \rangle - \frac{1}{2} \cdot \langle \Psi^f | \hat{V}^R | \Psi^f \rangle \quad (54)$$

$$\langle \Psi^f | \hat{V}^R | \Psi^f \rangle = \int V(\vec{r}) \cdot \rho(\vec{r}) \cdot d^3\vec{r} \quad (55)$$

### 3- Results and discussion

#### 3-1- Comparison with other work

The only theoretical study directly related to this work is the one published in 2002 by Gier and all [5] in the gas phase. They report at the CASSCF/CASMP2 level the results of calculations on the structure and vibrations of gaseous (1,2,3-trihydroxybenzene) in the ground and excited state. The essential results that can be compared with the ours are given in table (1) for the planar structure of (1,2,3-trihydroxybenzene).

Bond lengths (Å) & angles (Degrees)	Our work	Gier [5]	Bond lengths (Å) & angles (Degrees)	Our work	Gier [5]
$C_1 - O_1$	1,383	1,363	$C_5 - C_6$	1,404	1,397
$O_1 - H_1$	0,971	0,942	$\Delta_1$	109,5	115,36
$C_2 - O_2$	1,380	1,360	$\theta_1$	124,8	111,29
$O_2 - H_2$	0,974	0,945	$\Delta_2$	117,6	117,80
$C_3 - O_3$	1,368	1,352	$\theta_2$	107,6	109,77
$O_3 - H_3$	0,975	0,945	$\Delta_3$	120,4	119,62
$C_1 - C_2$	1,402	1,393	$\theta_3$	107,3	109,52
$C_1 - C_6$	1,402	1,390			

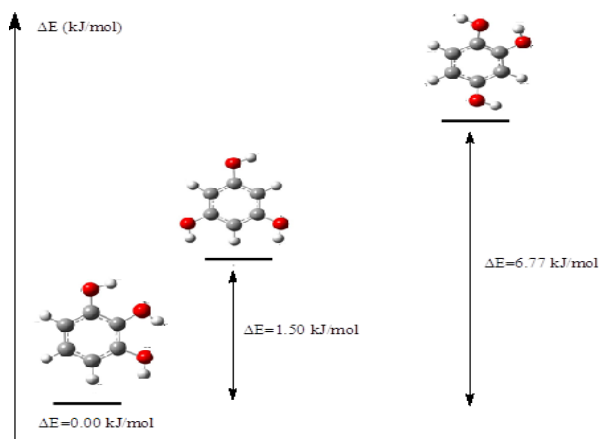
examination of the results shows that there is an excellent agreement between our DFT bond lengths and the one obtained by Gier by the CASSCF method. For the valence angles, the agreement is less, but we find that the agreement is generally very good for 4 of the 6 angles.

### 3-2- Energy and relative stability of isomers in the gas and solution phases

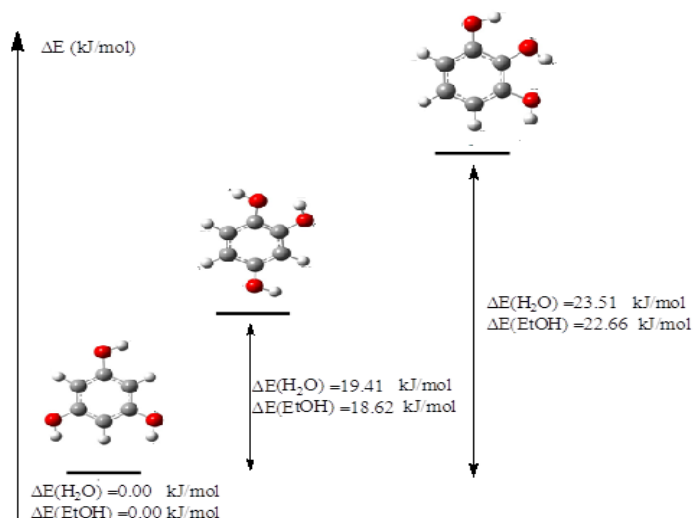
The relative energy values calculated relatively to the most stable molecule of the three hydroxyl benzene isomers in the gas and solution phases are reported in Table (2). The energy diagrams are reported in schemes (1) and (2).

**Table (2): Relative energy (kJ/mol) of trihydroxybenzene isomers in the gas and solution phases**

Isomers of three hydroxyl benzen									
	Gaz	H <sub>2</sub> O	EtOH	Gaz	H <sub>2</sub> O	EtOH	Gaz	H <sub>2</sub> O	EtOH
O1-H1	0.975	0.985	0.983	0.972	0.991	0.989	0.991	0.987	0.983
O2-H2	0.974	0.985	0.983	0.972	0.991	0.989	0.983	0.996	0.989
O3-H3	0.971	0.991	0.989	0.972	0.991	0.989	0.989	0.987	0.983
$\Delta E$ (kJ/mol)	0.00	23.51	22.66	1.50	0.00	0.00	6.77	19.41	18.62



**Scheme 1: Relative stability of isomers in the gas phase**



**Scheme (2): Relative stability of the isomers in the aqueous and alcoholic phases**

these results show that the 1,2,3-trihydroxybenzene isomer (we write 1,2,3 for abbreviation) is the most stable in the gas phase, because the intra molecular hydrogen bonds are considered, in this case, more stabilizing than for the other two isomers. This due to the position of the three OH groups in the molecule, that is the geometry and structure. While the 1,3,5 isomer becomes the most stable in the liquid phase, while the 1,2,3 isomer passing to the least stable order in the liquid phase. Therefore, the solvent provides stability for isomers, because as the 1,3,5-isomer passing from the second to the first order, and the 1,2,4-isomer passing from the third to the second order, while the 1,2,3 isomer pass from the first to the third order. We can interpret the first-place stability of 1,3,5 isomer by their possession of symmetry elements that reinforce the formation of hydrogen bonds suitable for more stability of the isomer.

### 3-3 IR spectra in the gas and solution phases

The O-H bond vibration frequencies and IR absorption intensity for both gas and solution phases of the studied isomers was reported in the table (2).

**Table (3): The DFT/B3LYP values of the absorption intensity and vibration frequency of the trihydroxybenzene isomers in the gas and solution phases**

						
	$\nu$ O-H <sub>i</sub> (cm <sup>-1</sup> )	Int. (KM/Mole)	$\nu$ O-H <sub>i</sub> (cm <sup>-1</sup> )	Int. (KM/Mole)	$\nu$ O-H <sub>i</sub> (cm <sup>-1</sup> )	Int. (KM/Mole)
Gas phase	3816 (O-H3) 3774 (O-H2) 3754 (O-H1)	73 98 88	3801 (O-H3) 3800 (O-H2) 3798 (O-H1)	66 26 61	3821 (O-H1) 3802 (O-H3) 3751 (O-H2)	66 55 95
Aqueous phase	3537(O-H1) 3523 (O-H2) 3379 (O-H3)	357 370 502	3394 (O-H1) 3386 (O-H3) 3375 (O-H2)	228 693 366	3379 (O-H1) 3392 (O-H3) 3542 (O-H2)	666 245 350
Ethanol solvent	3589 (O-H1) 3580 (O-H2) 3419 (O-H3)	306 324 459	3426 (O-H3) 3422 (O-H1) 3416 (O-H2)	189 625 350	3416 (O-H1) 3429 (O-H3) 3596 (O-H2)	606 277 299

The results in table (3) shows a systematic decrease in the values of the frequencies of the O-H bonds when passing from the gas to the solution phase. This decrease can be explained by the inhibition of hydrogen bonds formed in the liquid phase to the vibration motion of the bonds, which, in turn, vibrate freely in the gas phase. We also notice a very important increase in the intensity of light absorption when passing from the gas to the liquid phase. This can be explained by the compression of the energy levels as a result of the energy stability resulting from the formation of hydrogen bonds that have for tertiary hydroxybenzene actions that contribute to more energy stability. On the other hand, our theoretical calculations confirm that the 1,2,3 isomer is unstable in water due to the nodal vibration frequency of O2-H2, which is -40 cm<sup>-1</sup>, and is then a transitional state. If we follow the dynamics of the accompanying vibrational motion for the negative frequency, we notice that O2-H2 does not want to stay in the plane and wants to get out of it. Figure (4) shows the frequency of the nodal vibration of the transition state

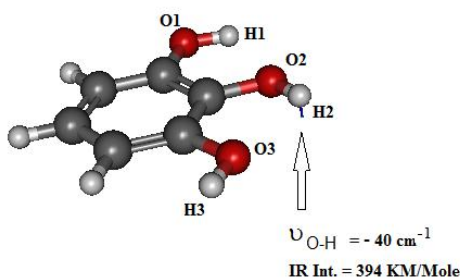


**Figure 4:** The nodal vibration frequency  $-40 \text{ cm}^{-1} = \nu_{\text{O2-H2}}$  for the transition state.

We show in table (4) our DFT/B3LYP/Toulouse pseudo potential Basis set and other theoretical CASSCF [5] and DFT/B3LYP [45] calculations of IR frequencies of OH groups in the 1,2,3 isomer (Pyrogallol), compared to the experimental one [45]. In 2018, Selvaraj and all [45] published an experimental and theoretical study on the pyrogallol. They investigate an experimental vibrational analysis of pyrogallol in solid phase by FT-IR and FT Raman spectroscopic techniques in the region  $4000\text{-}400 \text{ cm}^{-1}$  and  $4000\text{-}40 \text{ cm}^{-1}$ , respectively. Furthermore, they report the optimized molecular geometry, wave number and intensity of the vibrational bands of pyrogallol obtained by DFT method with different basis sets. In 2018, Ramasamy [46] investigate the molecular vibrations of pyrogallol by FT-IR and FT-Raman spectroscopies and report the experimental values of O-H stretching of the three OH groups. Already we constate that the experimental values obtained by FT-IR technique are very close for the two reference [45] and [46]. By comparing our results with that of Gier and all [5], we see that DFT/B3LYP provides the correct order of magnitude with however a limited deviation from the values of the more precise CASSCF method. On the other hand, the DFT/B3LYP/Toulouse pseudo potential method provides the correct classification of these frequencies. In addition, our results are relatively close to those of Selvaraj B3LYP results with other bases set, with relatively small deviations due to the effect of the base. On the other hand, globally the B3LYP results of Selvaraj differ notably from those of the CASSCF method. The only experimental value available for the vibration frequency of one of the OH groups shows that the three theoretical methods deviate from the experimental one, but the CASSCF method remains the most accurate.

**Table (4):** Our IR DFT/B3LYP/Toulouse pseudo potential, CASSCF [5], B3LYP [45] and experimental [45,46] frequencies of O-H<sub>i</sub> in 1,2,3 isomer (Pyrogallol)

$\nu \text{ O-H}_i (\text{cm}^{-1})$	Gas phase						Solid Phase	
	Our work	CASSCF	B3LYP/ 6-31 G(d,p)	B3LYP/ 6-31+ G(d,p)	B3LYP/ 6-311G (d,p)	B3LYP/ 6-311+G (d,p)	Exp: FT-IR	Exp: FT-IR
(O-H3)	3816	3663	3847	3849	3854	3854	-	3589
(O-H2)	3774	3609	3827	3832	3836	3838	-	3431
(O-H1)	3754	3601	3785	3790	3791	3793	3416	3401

In Figures (5-12) we report the infrared absorption spectra of the isomers of trihydroxybenzene in the gas phase, in water solution and in ethanol.

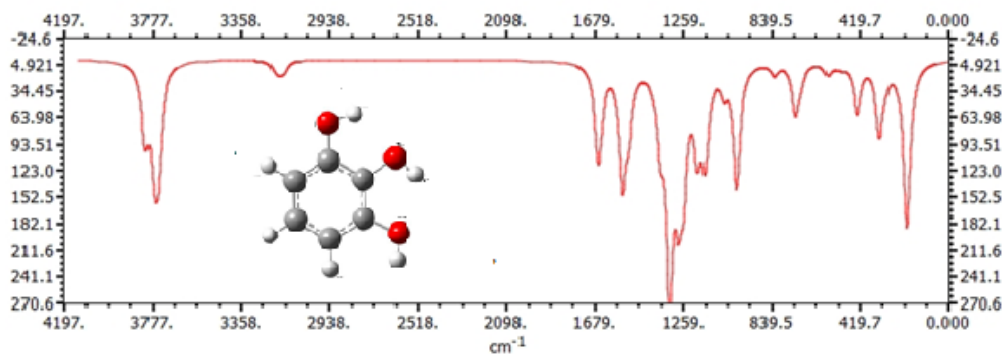


Figure 5: DFT/B3LYP absorption spectrum of the 1,2,3-trihydroxybenzene in the gas phase.

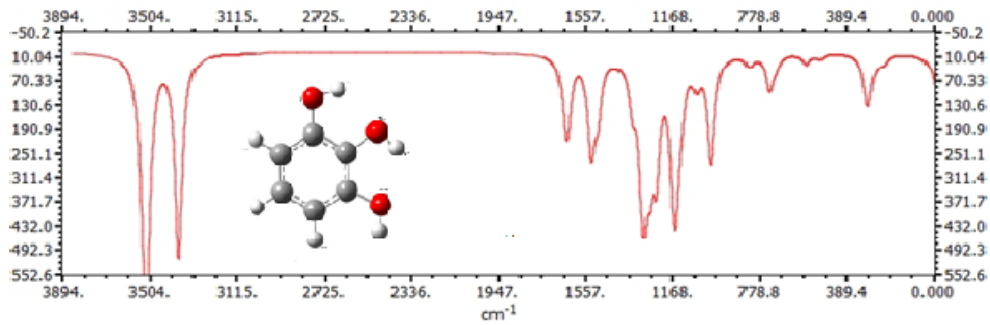


Figure 6: DFT/B3LYP absorption spectrum of the 1,2,3-trihydroxybenzene isomer in a solution of water.

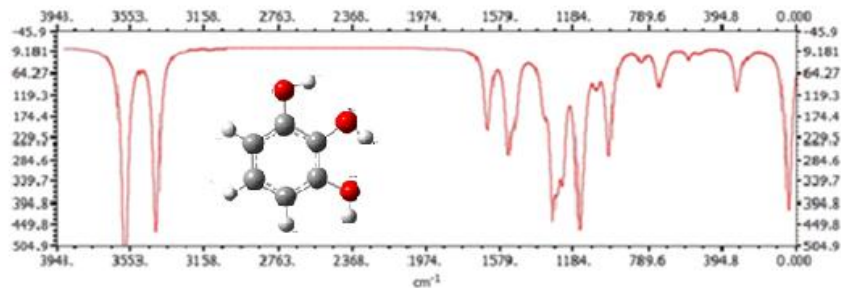


Figure 7: DFT/B3LYP absorption spectrum of the 1,2,3-trihydroxybenzene in ethanol solution.

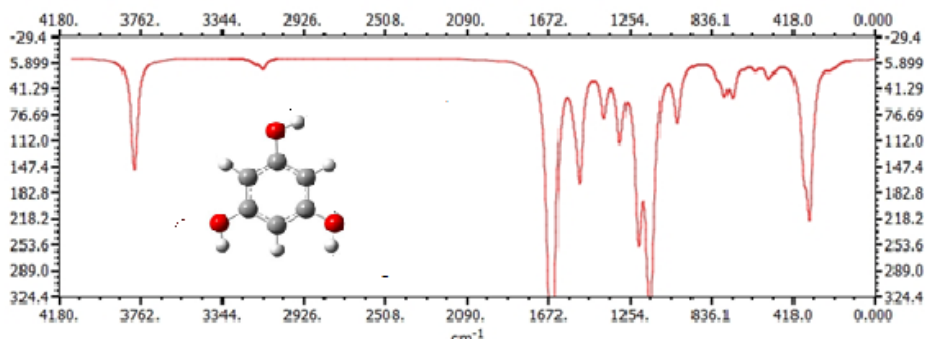


Figure 8: DFT/B3LYP absorption spectrum of the 1,3,5-trihydroxybenzene in the gas phase

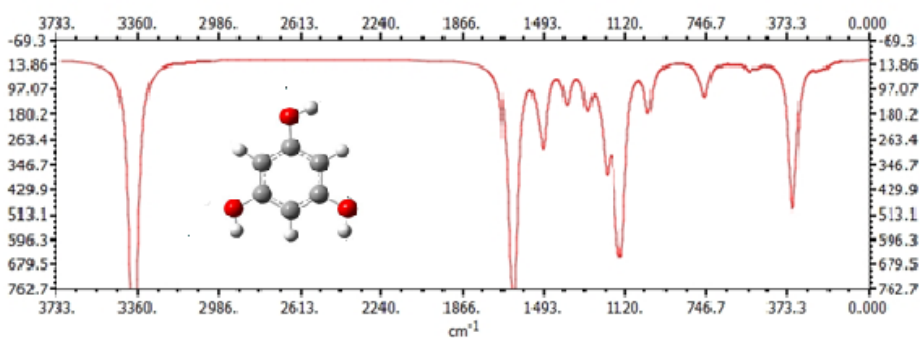


Figure 9: DFT/B3LYP absorption spectrum of the 1,3,5-trihydroxybenzene isomer in a solution of water.

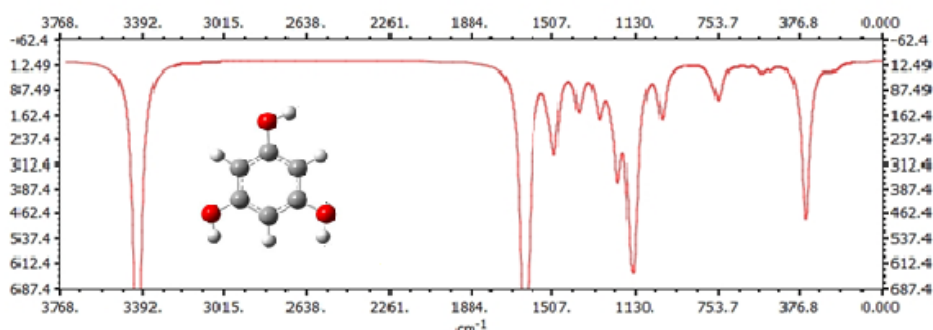


Figure 9: DFT/B3LYP absorption spectrum of the 1,3,5-trihydroxybenzene in ethanol solution.

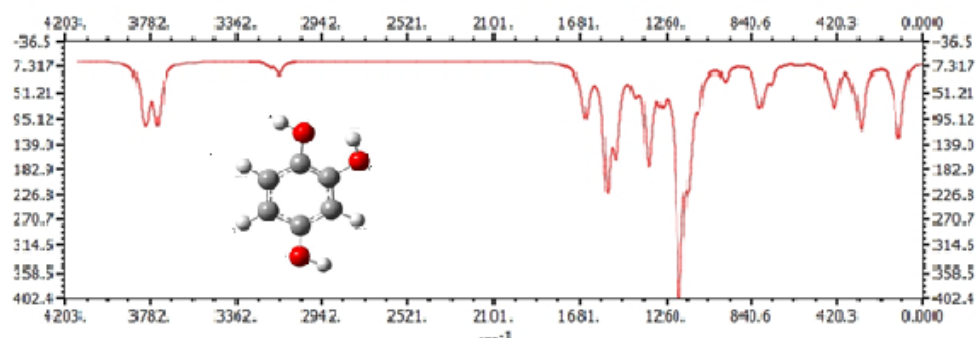


Figure 10: DFT/B3LYP absorption spectrum of 1,2,4-trihydroxybenzene in the gas phase

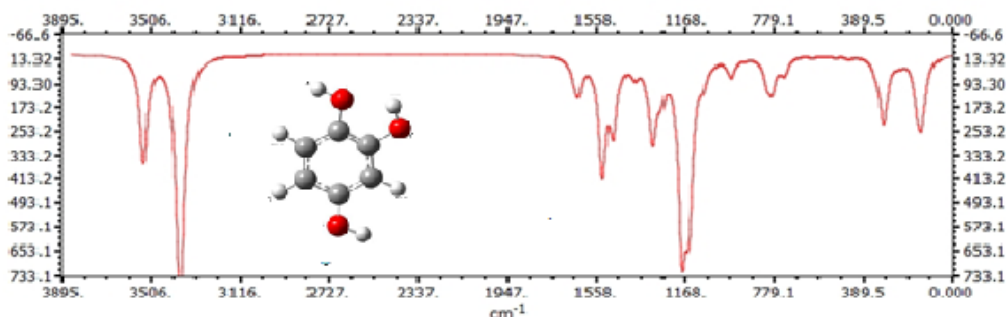


Figure 11: DFT/B3LYP absorption spectrum of the 1,2,4-trihydroxybenzene isomer in a solution of water

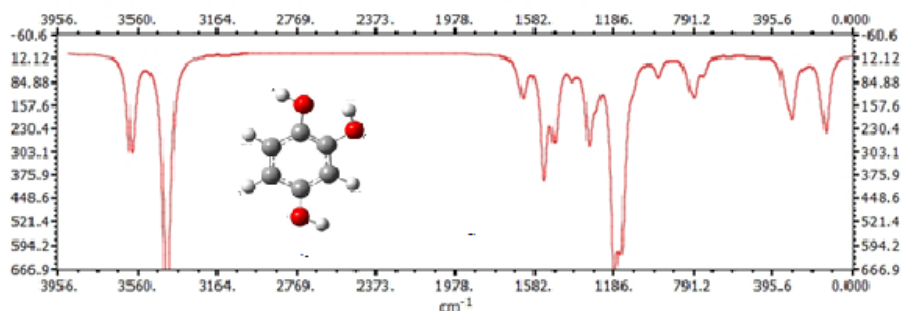


Figure 12: DFT/B3LYP absorption spectrum of the 1,2,4-trihydroxybenzene in ethanol solution.

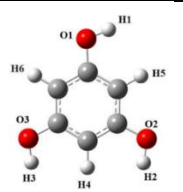
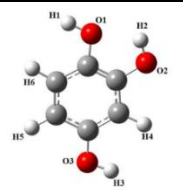
As noted in Table (2) for all isomers, we notice a clear increase in the absorption intensity when passing from the gas phase to the liquid phase. In addition, the role of the symmetry group elements of the molecules is also evident. The important role of the solvent on the intensity of absorption is also shown. For example, for the most stable 1,3,5 isomer in the liquid phase, we see that the absorption intensity of the O3-H3 bond is much greater than that of O1-H1 and O2-H2 in water, while the intensity of absorption of O1-H1 becomes greater than that of O2-H2. and O3-H3 in ethanol. Furthermore, we do not find the same behavior when passing from 1,3,5 to 1,2,4 in the gas and liquid phases. We conclude that the IR spectrums in the two compounds (1) and (3) observe the appearance of two bands in the specific region of the hydroxyl group. We

can interpret this by the presence of internal and external hydrogen bonds in both compounds. On the other hand, we observe from the spectrum of the compound (2) the existence of one absorption band, that we can interpret by the fact that the three-hydroxyl group are more distant one to other, fact that leads to weakness of the intra molecular hydrogen bonds.

3-4 Characteristic energies of the phenomenon of solvation:

We report in Table (3) the values of the total energy  $G_{total}$  and the energy difference between the solute and the Solvent  $G_{Solute}-G_{Solvent}$ , and the energy of confinement in cavity  $G_{Cavitation}$ , dispersion energy  $G_{Dispersion}$ , repulsion energy  $G_{Repulsion}$ , the non-electrostatic energy  $G_{Non Electrostatic}$ , and the self-consistent field energy including the energies comes from the PCM model  $E_{SCF+PCM}$ .

**Table (5): The values of the total energy, the energy difference between the solute and solvent, the energy of confinement in cavity, the scattering energy, the repulsion energy, the non-electrostatic energy and the SCF energy including energies comes from PCM model.**

						
Solvent	Water	Ethanol	Water	Ethanol	Water	Ethanol
$G_{total}$ (a.u.)	-85.555564	-85.558775	-85.564393	-85.567677	-85.557044	-85.560328
$G_{Solute}-G_{Solvent}$ (kcal/mol)	-17.25	-15.33	-24.67	-22.67	-20.28	-18.40
$G_{Cavitation}$ (kcal/mol)	18.23	13.31	18.38	13.42	18.32	13.38
$G_{Dispersion}$ (kcal/mol)	-14.43	-12.70	-14.63	-12.88	-14.54	-12.79
$G_{Repulsion}$ (kcal/mol)	1.33	1.10	1.46	1.21	1.40	1.16
$G_{Non Electrostatic}$ (kcal/mol)	5.13	1.71	5.21	1.75	5.18	1.74
$E_{SCF+PCM}$ (a.u.)	-85.563742	-85.561503	-85.572696	-85.570473	-85.565303	-85.563102

We show from Table (5) that the difference between the energy of the solute and the solvent is consistent with the relative energy stability of the isomers. We see also that for the three isomers the cavitation energy takes very close values in the same phase (aqueous or alcoholic). As example, we find, respectively, in water the values 18.38, 18.32 and 18.23 for the 1,3,5 and 1,2,4 and 1,2,3 isomers. We also find that there is an appreciable difference between the  $C_{Cavitation}$  value in water and in ethanol for the same isomer. This highlights the effects of the physical and structural properties of the dissolved medium on the cavitation energy. The same observation can be made regarding the scattering energy, but we find that the differences are less intense. On the other hand, the repulsion energy takes for different isomers close values in both aqueous or alcoholic media due to the structural belonging of these two solvents to the same family

$R - \underline{O} - H$ . Regarding the non-electrostatic energy, we note that it has the same behavior as the scattering energy in terms of numerical variation of the values, but it is of different numerical order

#### 4- Conclusion

In this paper, isomers of trihydroxybenzene were studied in the gas and solution phases using the density function theory DFT/B3LYP. Molecular geometry, energies of the isomers, their relative stability, theoretical infrared absorption spectra, all the energies related to the PCM model of solvation and all energies of isomers and their relative energies including the correction from the solvent action have been carried out quantum mechanically using the DFT/B3LYP method. This study has been showed without ambiguity the

important effect and role of the solvent action on the stability of the isomers and their structural and spectral properties and that no accurate quantitative study of a physicochemical problem could be carried out without taking into account the role of the solvent medium.

**References:**

1. Garde-Cerdán, Teresa; Gonzalo-Diago, Ana; Pérez-Álvarez, Eva P., 2017, Phenolic compounds: types, effects, and research, Nova Science Publishers.
2. Vermerris W., Nicholson R., 2006, Phenolic Compounds Biochemistry, springer
3. Collin M. Mayhan, Harshita Kumari, Julia M. Maddalena, Gabriel N. Borgmeyer & Carol A. Deakyne, (2021), Proton affinity and gas-phase basicity of pyrogallol and phloroglucinol: a computational study, JOURNAL OF COORDINATION CHEMISTRY, VOL. 74, NOS. 1–3, 61–73
4. Kgalaletso P. Otukile and Mwadham M. Kabanda , (2019), A DFT mechanistic, thermodynamic and kinetic study on the reaction of 1, 3, 5-trihydroxybenzene and 2, 4, 6-trihydroxyacetophenone with  $\bullet\text{OOH}$  in different media ,Journal of Theoretical and Computational Chemistry Vol. 18, No. 4,1950023
5. H. Gier, W. Roth, S. Schumm, M. Gerhards, (2002), Structures of 1,2,3-trihydroxybenzene in the  $S_0$  and  $S_1$  states, Journal of Molecular Structure, 610, 1-16.
6. Rashed Taleb Rashee, Mahammed Shamil Ali, Hadeel Salah Mansoor, Hasan R. Obayes, Abdalnasser M. AL-Gebori. (2015), Synthesis and Theoretical Study of Some 2,4,6 Trihydroxyacetophenone Schiff base Ligandes, Eng. &Tech.Journal, Vol.33, Part (B), No.1.
7. Julian Tirado-Rives and William L. Jorgensen, (2008), Performance of B3LYP Density Functional Methods for a Large Set of Organic Molecules, J. Chem. Theory Comput., 4, 297-306
8. Bouteiller, Y. ; Mijoule C. ; Nizam M. ; Barthelat, J.-C. ; Daudey, J. P. ; Pelissier, M. M.; Silvi, B. , (1988), Extended gaussian-type valence basis sets for calculations involving non-empirical core pseudopotentials. Molecular Physics, 65. 295-312
9. McWeeny, R., 1992, Methods of Molecular Quantum Mechanic
10. Yamanouchi, K., 2013, Quantum Mechanics of Molecular Structures, Springer-Verlag Berlin and Heidelberg
11. Morin, J. and Pelletier, J. M., 2013, Density Functional Theory: Principles, Applications and Analysis (Physics Research and Technology),
12. Roy, A. K., 2013, Theoretical and Computational Developments in Modern Density Functional Theory (Physics Research and Technology),
13. Engel, E., Dreizler, R. M., 2011, Density Functional Theory\_ (Theoretical and Mathematical Physics), Springer-Verlag Berlin Heidelberg.
14. Dreizler, R.M., Gross, E.K.U., 1996, Density functional theory: an approach to the quantum many-body problem, springer.
15. Parr, R. G., Yang, W., 1994, Density-functional theory of atoms and molecules, Oxford University Press.
16. Gill, P. M. W., Johnson, B. G., Pople, J. A., and Frisch, M. J., 1992, "The performance of the Becke-Lee-Yang-Parr (B-LYP) density functional theory with various basis sets," Chem. Phys. Lett., 197, 499-505.
17. Bartolotti, L. J., Flurchick, K., 1996, An introduction to density functional theory, Rev. Comput. Chem., 7, 187-216.
18. St-Amant, A., 1996, Density functional methods in biomolecular modeling, Rev. Comput. Chem., 7, 217.
19. Ziegler, T., 1991, Approximate density functional theory as a practical tool in molecular energetics and dynamics , Chem. Rev., 91 (5), 651-667.
20. Baerends, E., Gritsenko, O. V., 1997, A Quantum Chemical View of Density Functional Theory, J. Phys. Chem. A, 101 (30), 5383-5403.
21. Andzelm, J., and Wimmer, E., 1992, "Density functional Gaussian-type-orbital approach to molecular geometries, vibrations, and reaction energies," J. Chem. Phys., 96, 1280-303.
22. Hohenberg, P. and Kohn, W., 1964, "Inhomogeneous Electron Gas," Phys. Rev., 136 B864-B71.
23. Kohn, W. and Sham, L. J., 1965, "Self-Consistent Equations Including Exchange and Correlation Effects," Phys. Rev., 140 A1133-A38.
24. Vosko, S. J., Wilk, L., Nusair, M., 1980, Accurate spin-dependent electron liquid correlation energies for local spin density calculations: a critical analysis , Can. J. Phys., 58 (8), 1200-1211.
25. Jensen, F., 1999, Introduction to Computational Chemistry, John Wiley & Sons.
26. Becke, A. D., 1988, Phys. Rev., B38, 3098.
27. Becke, A. D., 1992, "Density-functional thermochemistry. I. The effect of the exchange-only gradient correction," J. Chem. Phys., 96, 2155-60.

28. Becke, A.D., 1992, "Density-functional thermochemistry. II. The effect of the Perdew-Wang generalized-gradient correlation correction.", J. Chem. Phys., 97, 9173-77.
29. Perdew, J. P. and Wang, Y., 1986, Accurate and simple density functional for the electronic exchange energy: Generalized gradient approximation, Phys. Rev., B33, Issue 12, 8800.
30. Perdew, J. P. and Wang, Y., 1992, "Accurate and Simple Analytic Representation of the Electron Gas Correlation Energy", Phys. Rev. B, 45, 13244-49.
31. Lee, C., Yang, W., Parr, R. G., 1988, Development of the Colle-Salvetti correlation-energy formula into a functional of the electron density, Phys. Rev., B37, 785.
32. Becke, A. D., 1993, Density-functional thermochemistry. III. The role of exact exchange, J. Chem. Phys., 98, 5648.
33. Kirkwood, J.G., 1934, Theory of solutions of molecules containing widely separated charges with special application to amphoteric ions, J. Chem. Phys., 2, 351-61
34. Baldrige, K., Klant, A., 1997, First principles implementation of solvent effects without outlying charge error, J. Chem. Phys., 106 (16), 6622-6633
35. Onsager, L., 1936, Electric Moments of Molecules in Liquids, J. Am. Chem. Soc., 58 (8), 1486-1493.
36. Cossi, M., Mennucci, B., Pitarch, J., Tomasi, J., 1998, Correction of cavity-induced errors in polarization charges of continuum solvation models, J. Comp. Chem., 19, 833-846.
37. Miertus, S., Scrocco, E., Tomasi, J., 1981, Electrostatic interaction of a solute with a continuum. A direct utilization of AB initio molecular potentials for the prevision of solvent effects, J. Chem. Phys., 55, Issue 1, 117-129.
38. Tomasi, J., Persico, M., 1994, Molecular Interactions in Solution: An Overview of Methods Based on Continuum Distributions of the Solvent, Chem. Rev., 94(7), 2027-2094.
39. Cammi, R., Tomasi, J., 1995, Remarks on the use of the apparent surface charges (ASC) methods in solvation problems: Iterative versus matrix-inversion procedures and the renormalization of the apparent charges, J. Comp. Chem., 16, Issue 12, 1449-1458.
40. Miertus, S., Scrocco, E., Tomasi, J., 1981, Electrostatic interaction of a solute with a continuum. A direct utilization of AB initio molecular potentials for the prevision of solvent effects, Chemical Physics, 55, Issue 1, 117-129.
41. Pierotti, R. A., 1976, A scaled particle theory of aqueous and nonaqueous solutions, Chem. Rev., 76, 717-726.
42. Langlet, J., Claverie, P., Caillet, J., Pullman, A., 1988, Improvements of the continuum model. 1. Application to the calculation of the vaporization thermodynamic quantities of nonassociated liquids, J. Phys. Chem., 92 (6), 1617-1631.
43. Lennard-Jones, J. E. C., 1931, Proceeding of Physical Society, 43, 461.
44. Floris, F., Tomasi, J., 1989, Evaluation of the dispersion contribution to the solvation energy. A simple computational model in the continuum approximation, J. Comput. Chem., 10, Issue 5, 616-627.
45. S. Selvaraj a,\*, P. Rajkumar a, K. Thirunavukkarasu a, S. Gunasekaran b, S. Kumaresan, Vibrational (FT-IR and FT-Raman), electronic (UV-Vis) and quantum chemical investigations on pyrogallol: A study on benzenetriol dimers, Vibrational Spectroscopy, Volume 95, March 2018, Pages 16-22
46. R. Ramasamy, (2016), Vibrational Assignments of FT-IR and FT-Raman Spectra of Pyrogallol, Int. Journal of Engineering Research and Application, ISSN: 2248-9622, Vol. 6, Issue 9, (Part -3) September 2016, pp.64-68